

Supporting Information

Mn²⁺-doped organic-inorganic hybrid (C₈H₂₀N)₂Zn_{1-x}Mn_xBr₄ as sub-micrometer green phosphor for Mini-LED/Micro-LED

Sixiang Wang,^a Yichang Wang,^a DaeHo Yoon,^b Tianrong Li,^{*a} and Yuhua Wang^{*a}

^a *School of Materials and Energy, National and Local Joint Engineering Laboratory for Optical Conversion Materials, Lanzhou University, Lanzhou 730000, China*

^b *School of Advanced Materials Science & Engineering, Sungkyunkwan University, Suwon 16419, Korea.*

*Corresponding authors.

E-mail addresses: litr@lzu.edu.cn (Tianrong Li), wyh@lzu.edu.cn (Yuhua Wang).

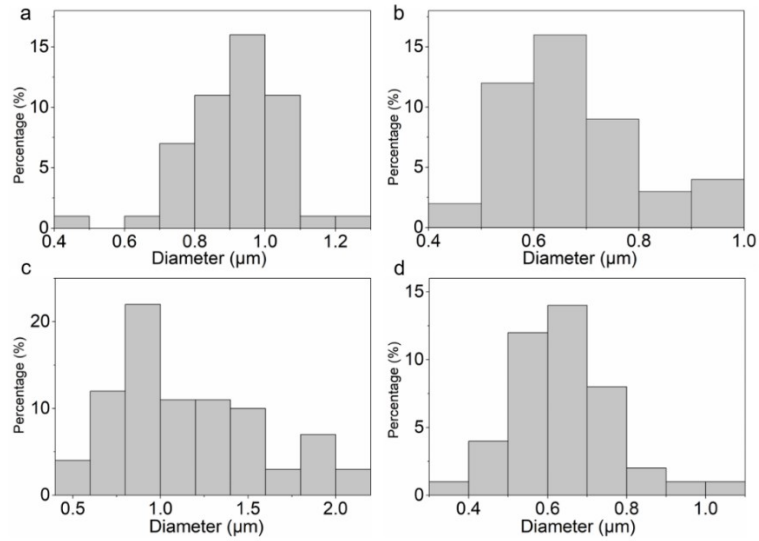


Figure S1. Size distribution of $(\text{C}_8\text{H}_{20}\text{N})_2\text{Zn}_{1-x}\text{Mn}_x\text{Br}_4$ (a) $x = 0$, (b) $x = 0.1$, (c) $x = 0.2$, and (d) $x = 0.3$.

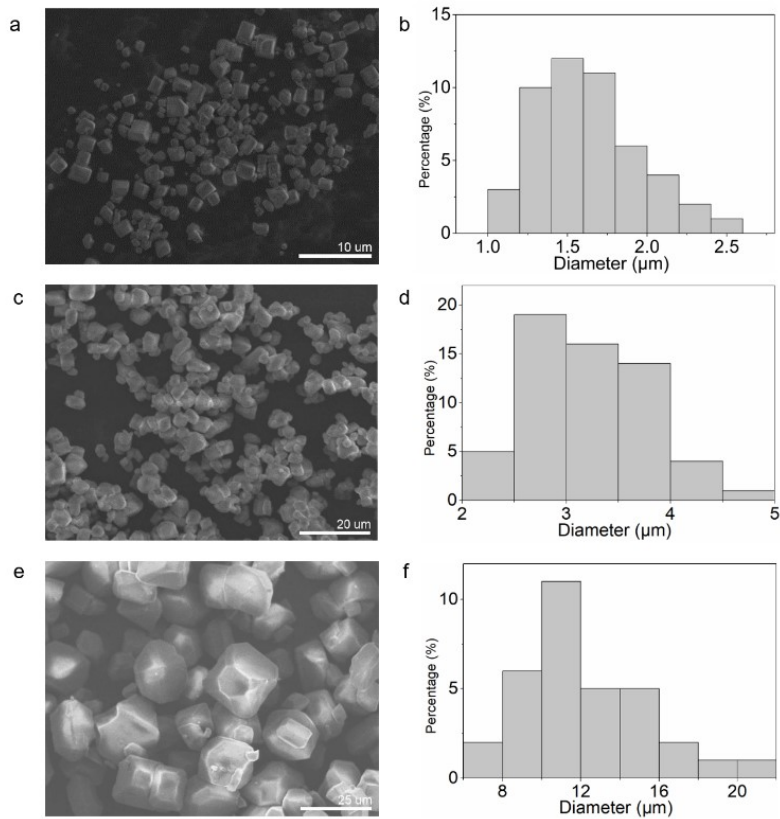


Figure S2. (a) SEM image and (b) size distribution of $(\text{C}_8\text{H}_{20}\text{N})_2\text{MnBr}_4$. (c) SEM image and (d) size distribution of $(\text{C}_8\text{H}_{20}\text{N})_2\text{Zn}_{0.2}\text{Mn}_{0.8}\text{Br}_4$. (e) SEM image and (f) size distribution of $(\text{C}_8\text{H}_{20}\text{N})_2\text{Zn}_{0.5}\text{Mn}_{0.5}\text{Br}_4$.

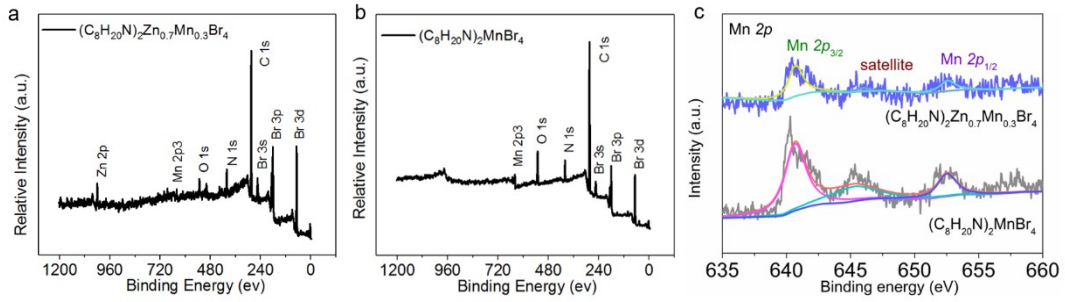


Figure S3. XPS survey spectra of (a) $(\text{C}_8\text{H}_{20}\text{N})_2\text{Zn}_{0.7}\text{Mn}_{0.3}\text{Br}_4$ and (b) $(\text{C}_8\text{H}_{20}\text{N})_2\text{MnBr}_4$. (c) HR-XPS spectra of $(\text{C}_8\text{H}_{20}\text{N})_2\text{Zn}_{0.7}\text{Mn}_{0.3}\text{Br}_4$ and $(\text{C}_8\text{H}_{20}\text{N})_2\text{MnBr}_4$ of Mn $2p$, the satellite peak also belongs to Mn^{2+}

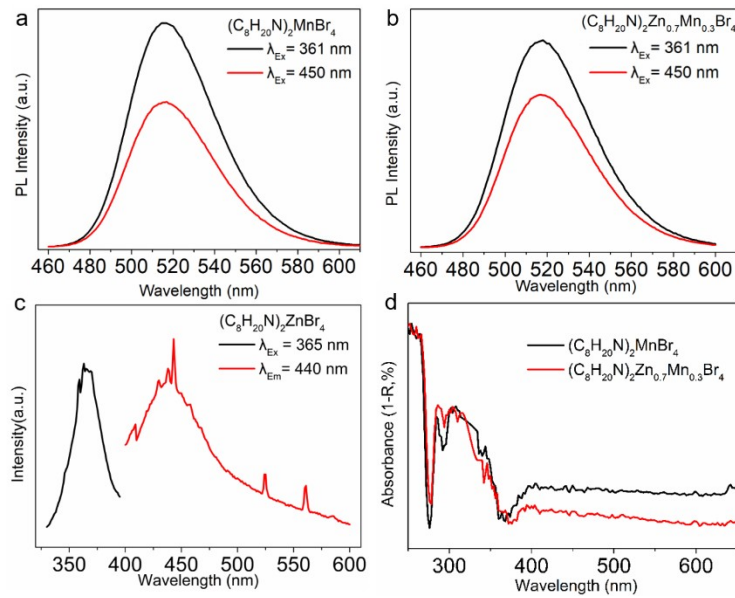


Figure S4. (a) PL spectra of $(\text{C}_8\text{H}_{20}\text{N})_2\text{MnBr}_4$ and (b) $(\text{C}_8\text{H}_{20}\text{N})_2\text{Zn}_{0.7}\text{Mn}_{0.3}\text{Br}_4$ triggered by different excitation wavelengths. (c) PL spectra of $(\text{C}_8\text{H}_{20}\text{N})_2\text{ZnBr}_4$. (d) Absorption spectra of $(\text{C}_8\text{H}_{20}\text{N})_2\text{MnBr}_4$ and $(\text{C}_8\text{H}_{20}\text{N})_2\text{Zn}_{0.7}\text{Mn}_{0.3}\text{Br}_4$

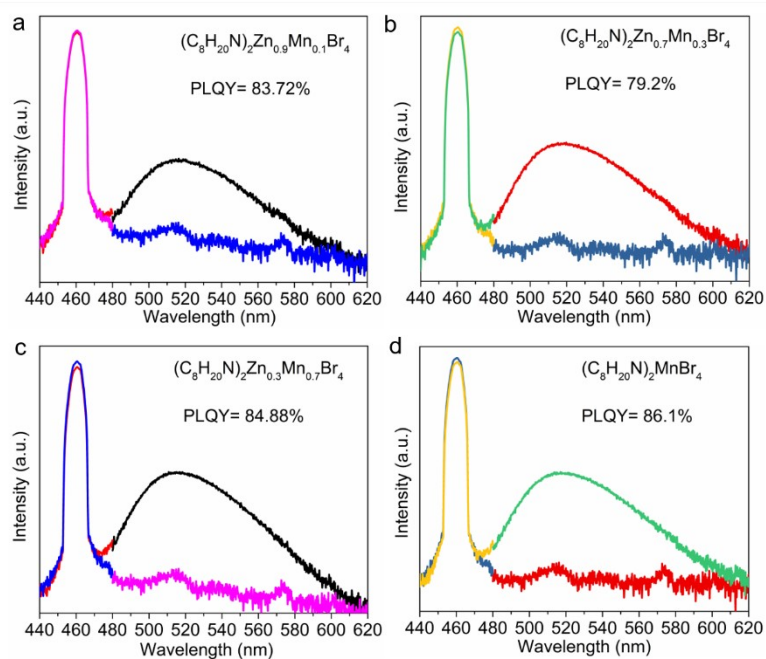


Figure S5. PLQY results of $(\text{C}_8\text{H}_{20}\text{N})_2\text{Zn}_{1-x}\text{Mn}_x\text{Br}_4$ ($x = 0.1, 0.3, 0.7,$ and 1.0) at 460 nm excitation.

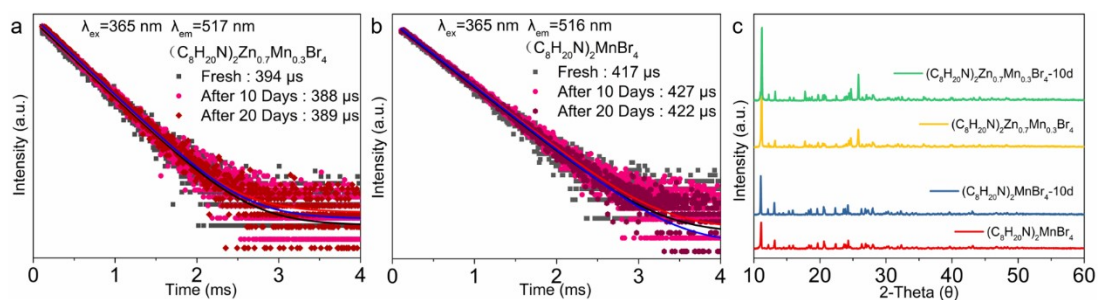


Figure S6. Decay curves of (a) $(\text{C}_8\text{H}_{20}\text{N})_2\text{Zn}_{0.7}\text{Mn}_{0.3}\text{Br}_4$ and (b) $(\text{C}_8\text{H}_{20}\text{N})_2\text{MnBr}_4$ overtime during the stability experiments. (c) XRD patterns of $(\text{C}_8\text{H}_{20}\text{N})_2\text{Zn}_{0.7}\text{Mn}_{0.3}\text{Br}_4$ and $(\text{C}_8\text{H}_{20}\text{N})_2\text{MnBr}_4$ during the stability experiments.

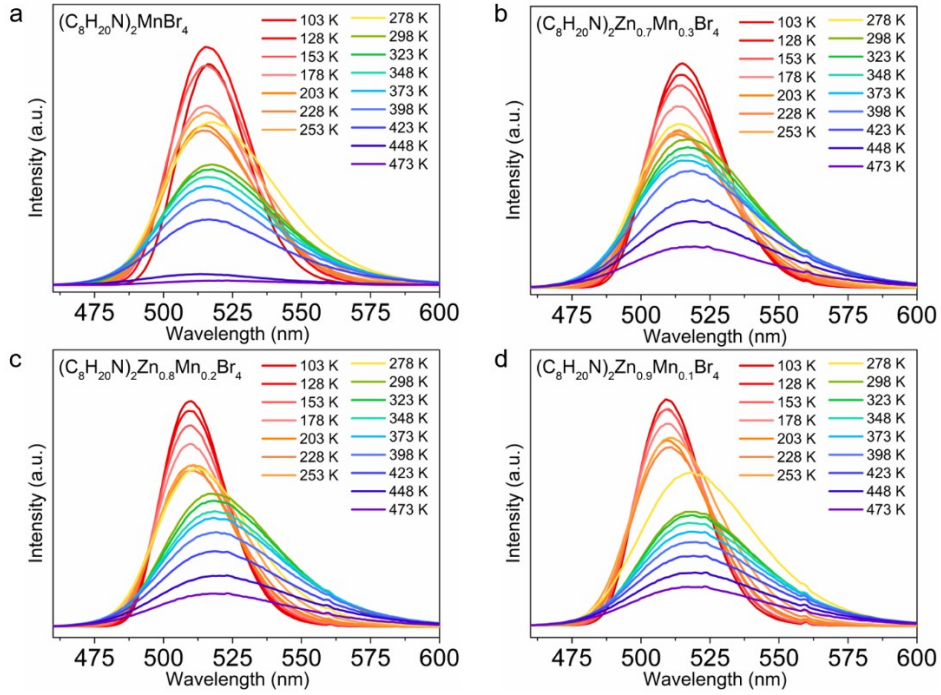


Figure S7. Temperature-dependent PL spectra of (a) $(\text{C}_8\text{H}_{20}\text{N})_2\text{MnBr}_4$, (b) $(\text{C}_8\text{H}_{20}\text{N})_2\text{Zn}_{0.7}\text{Mn}_{0.3}\text{Br}_4$, (c) $(\text{C}_8\text{H}_{20}\text{N})_2\text{Zn}_{0.8}\text{Mn}_{0.2}\text{Br}_4$ and (d) $(\text{C}_8\text{H}_{20}\text{N})_2\text{Zn}_{0.9}\text{Mn}_{0.1}\text{Br}_4$ ($T = 103\text{--}473\text{ K}$, $\lambda_{\text{ex}} = 361\text{ nm}$).

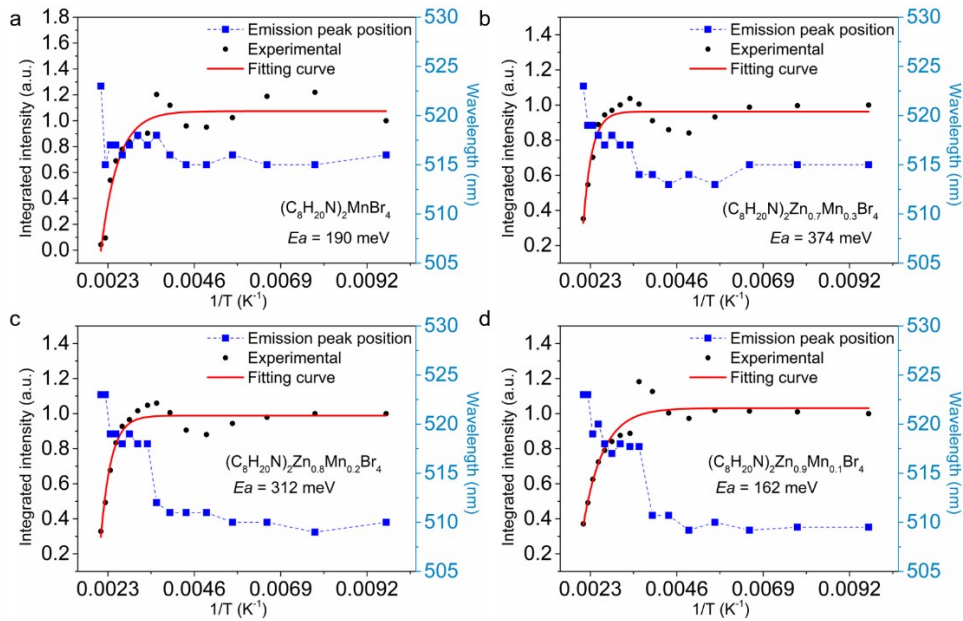


Figure S8. Temperature-dependent emission peak position and integrated PL intensity and the corresponding fitting curves of (a) $(\text{C}_8\text{H}_{20}\text{N})_2\text{MnBr}_4$, (b) $(\text{C}_8\text{H}_{20}\text{N})_2\text{Zn}_{0.7}\text{Mn}_{0.3}\text{Br}_4$, (c) $(\text{C}_8\text{H}_{20}\text{N})_2\text{Zn}_{0.8}\text{Mn}_{0.2}\text{Br}_4$ and (d) $(\text{C}_8\text{H}_{20}\text{N})_2\text{Zn}_{0.9}\text{Mn}_{0.1}\text{Br}_4$ in the range of $103 \sim 473\text{ K}$.

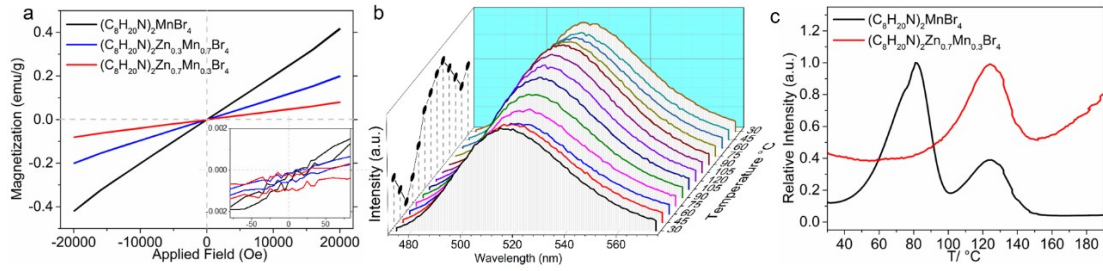


Figure S9. (a) M-H loops of $(\text{C}_8\text{H}_{20}\text{N})_2\text{Zn}_{1-x}\text{Mn}_x\text{Br}_4$ ($x = 0.3, 0.7, \text{ and } 1.0$). The inset shows the magnified area near the zero magnetic field of M-H loops. (b) Temperature-dependent PL spectra of $(\text{C}_8\text{H}_{20}\text{N})_2\text{MnBr}_4$ after being fully illuminated in the temperature range of $30\text{ }^\circ\text{C}$ to $120\text{ }^\circ\text{C}$ and $120\text{ }^\circ\text{C}$ to $30\text{ }^\circ\text{C}$. The inset shows the relative emission intensity at different temperatures. (c) Thermo-luminescent spectra of $(\text{C}_8\text{H}_{20}\text{N})_2\text{Zn}_{0.7}\text{Mn}_{0.3}\text{Br}_4$ and $(\text{C}_8\text{H}_{20}\text{N})_2\text{MnBr}_4$.

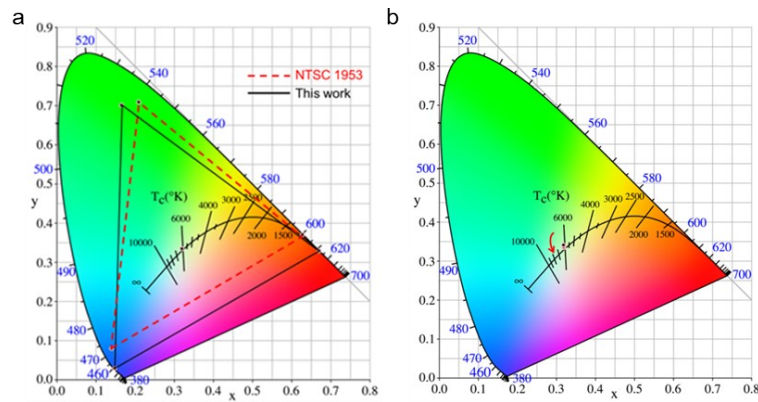


Figure S10. (a) Color gamut range $(\text{C}_8\text{H}_{20}\text{N})_2\text{Zn}_{0.7}\text{Mn}_{0.3}\text{Br}_4$ contrast NTSC standard. (b) The change of color coordinate of the WLED under different currents.

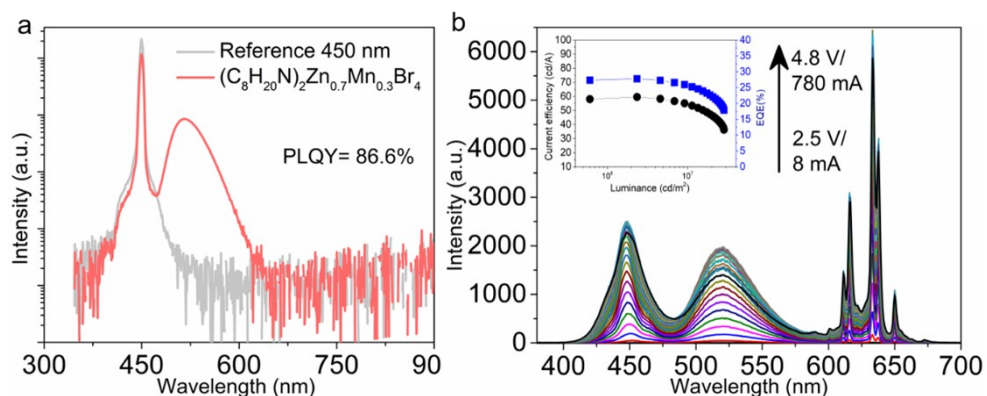


Figure S11. (a) PLQY of $(\text{C}_8\text{H}_{20}\text{N})_2\text{Zn}_{0.7}\text{Mn}_{0.3}\text{Br}_4$ powder under 450 nm excitation. (b) Electroluminescence spectra of the W-LED device under different power efficiencies. The inset shows the external quantum efficiency (EQE) versus luminance characteristics for WLED devices based on $(\text{C}_8\text{H}_{20}\text{N})_2\text{Zn}_{0.7}\text{Mn}_{0.3}\text{Br}_4$.

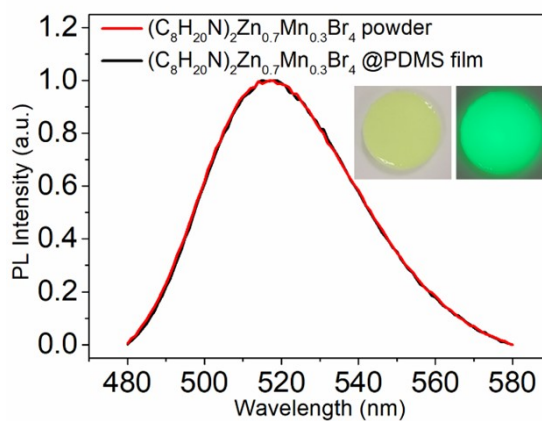


Figure S12. PL spectra of a flexible and luminescent film encapsulated by the $(\text{C}_8\text{H}_{20}\text{N})_2\text{Zn}_{0.7}\text{Mn}_{0.3}\text{Br}_4$ powder and polydimethylsiloxane (PDMS). Illustration: photos of the film under visible light and 365 nm light.

Table S1. Crystal data and structure refinement of $(C_8H_{20}N)_2Zn_{1-x}Mn_xBr_4$ ($x = 0, 0.3, 0.5,$ and 1)

Empirical formula	$(C_8H_{20}N)_2MnBr_4$	$(C_8H_{20}N)_2Zn_{0.5}Mn_{0.5}Br_4$	$(C_8H_{20}N)_2Zn_{0.7}Mn_{0.3}Br_4$	$(C_8H_{20}N)_2ZnBr_4$
Temperature/K	293	150	293	303
Crystal color	Green	Green	Green	Colorless
Crystal system	Tetragonal	Tetragonal	Tetragonal	Tetragonal
Space group	P -421m	P-421m	P42/n m c	P 42/n m c
a/Å	13.3908(6)	13.2487(2)	8.9998(4)	9.0097(5)
b/Å	13.3908(6)	13.2487(2)	8.9998(5)	9.0097(5)
c/Å	14.4477(9)	14.3725(5)	15.9725(7)	16.0020(10)
$\alpha/^\circ$	90	90	90	90
$\beta/^\circ$	90	90	90	90
$\gamma/^\circ$	90	90	90	90
Volume/Å ³	2590.7(3)	2522.78(12)	1293.7(11)	1298.96(17)

Table S2. Fractional Atomic Coordinates ($\times 10^4$) and Equivalent Isotropic Displacement Parameters ($\text{Å}^2 \times 10^3$) for $(C_8H_{20}N)_2Zn_{0.5}Mn_{0.5}Br_4$. U_{eq} is defined as 1/3 of the trace of the orthogonalized U_{ij} tensor.

Atom	x	y	z	$U(eq)$
Br01	8677.3(13)	6322.7(13)	6959.0(15)	30.4(5)
Br02	7555.8(13)	7444.2(13)	9474.8(16)	35.0(5)
Br03	5730.9(13)	7045.3(14)	7235.3(13)	37.4(4)
Mn04	7478.3(16)	7521.7(16)	7732.0(2)	23.2(6)
N005	5000.0	10000.0	-42(19)	27(5)
N006	7074.0	7926.0(9)	4209(12)	22(3)
N007	5000.0	5000.0	0	24(5)
C008	6242(13)	7468(13)	3633(11)	31(3)
C009	7890(15)	7110(15)	4457(19)	39(5)
C00A	5523(19)	6220(2)	1316(17)	56(5)
C00B	5687(16)	6577(15)	4096(14)	43(4)
C00C	8378(17)	6622(17)	3600(2)	48(7)
C00D	5923(14)	9077(14)	1293(18)	36(5)
C00E	6723(14)	8277(14)	5157(19)	37(5)
C00F	5900(2)	9100(2)	5080(3)	62(9)
N00G	9090(3)	5910(3)	1350(3)	109(15)
C00H	5910(2)	5340(2)	592(19)	60(6)

Atom	<i>x</i>	<i>y</i>	<i>z</i>	U(eq)
C00I	5070(3)	9020(3)	570(3)	98(11)

Table S3. Bond Lengths for (C₈H₂₀N)₂Zn_{0.5}Mn_{0.5}Br₄.

Atom	Atom	Length/Å
Br01	Mn04	2.506(4)
Br02	Mn04	2.509(4)
Br03	Mn04	2.503(2)
N005	C00I	1.56(4)
N005	C00I	1.56(4)
N005	C00I	1.56(4)
N005	C00I	1.56(4)
N006	C008	1.507(19)
N006	C008	1.507(19)
N006	C009	1.57(3)
N006	C00E	1.51(3)
N007	C00H	1.54(3)
N007	C00H	1.54(3)
N007	C00H	1.54(3)
N007	C00H	1.54(3)
C008	C00B	1.54(3)
C009	C00C	1.54(4)
C00A	C00H	1.65(4)
C00D	C00I	1.54(4)
C00D	C00I	1.54(4)
C00E	C00F	1.54(5)
C00I	C00I	1.96(8)
C00I	C00I	1.69(8)

Table S4. Bond Angles for (C₈H₂₀N)₂Zn_{0.5}Mn_{0.5}Br₄.

Atom	Atom	Atom	Angle/°	Atom	Atom	Atom	Angle/°
Br01	Mn04	Br02	112.99(14)	C00H	N007	C00H	107.7(10)
Br03	Mn04	Br01	107.45(9)	C00H	N007	C00H	113(2)
Br03	Mn04	Br01	107.45(9)	C00H	N007	C00H	113(2)
Br03	Mn04	Br02	108.19(9)	C00H	N007	C00H	107.7(10)
Br03	Mn04	Br02	108.19(9)	C00H	N007	C00H	107.7(10)
Br03	Mn04	Br03	112.64(14)	N006	C008	C00B	114.8(14)
C00I	N005	C00I	78(3)	C00C	C009	N006	113(2)
C00I	N005	C00I	112(3)	C00I	C00D	C00I	67(3)
C00I	N005	C00I	65(3)	N006	C00E	C00F	112(2)
C00I	N005	C00I	65(3)	N007	C00H	C00A	108.2(18)
C00I	N005	C00I	78(3)	N005	C00I	C00I	51.1(15)
C00I	N005	C00I	112(3)	N005	C00I	C00I	57.3(15)
C008	N006	C008	106.7(16)	C00D	C00I	N005	113(3)
C008	N006	C009	110.6(11)	C00D	C00I	C00I	119.1(17)
C008	N006	C009	110.6(11)	C00D	C00I	C00I	56.6(15)
C008	N006	C00E	113.1(11)	C00I	C00I	C00I	89.999(1)
C008	N006	C00E	113.1(11)	C00E	N006	C009	102.7(17)

Table S5. Torsion Angles for (C₈H₂₀N)₂Zn_{0.5}Mn_{0.5}Br₄.

A	B	C	D	Angle/°
C008	N006	C008	C00B	178.8(11)
C008	N006	C009	C00C	-59.0(11)
C008	N006	C009	C00C	59.0(11)
C008	N006	C00E	C00F	60.8(12)
C008	N006	C00E	C00F	-60.8(12)
C009	N006	C008	C00B	58.5(19)
C009	N006	C00E	C00F	179.999(8)
C00E	N006	C008	C00B	-56(2)
C00E	N006	C009	C00C	179.999(5)
C00H	N007	C00H	C00A	-173.4(19)
C00H	N007	C00H	C00A	64.4(10)
C00H	N007	C00H	C00A	-54.5(14)
C00I	N005	C00I	C00D	-53(2)

C00I	N005	C00I	C00D	11(3)
C00I	N005	C00I	C00D	-110(2)
C00I	N005	C00I	C00I	121(2)
C00I	N005	C00I	C00I	57(2)
A	B	C	D	Angle/°
C00I	N005	C00I	C00I	-121(2)
C00I	N005	C00I	C00I	-64.3(17)
C00I	C00D	C00I	N005	-11(3)
C00I	C00D	C00I	C00I	-68.4(17)

Table S6. Fractional Atomic Coordinates ($\times 10^4$) and Equivalent Isotropic Displacement Parameters ($\text{\AA}^2 \times 10^3$) for $(\text{C}_8\text{H}_{20}\text{N})_2\text{ZnBr}_4$. U_{eq} is defined as 1/3 of the trace of the orthogonalised U_{IJ} tensor.

Atom	x	y	z	$U(\text{eq})$
Zn01	2500	7500	2500	55.7(6)
Br02	2500	5330.1(13)	1625.5(7)	100.9(6)
N003	2500	2500	4145(5)	65(2)
C004	2500	4788(16)	5048(10)	156(8)
C006	2500	4230(30)	4175(14)	96(6)
C2	2500	2500	4970(20)	208(16)
C1	-50(40)	2500	3420(30)	168(14)
C3	830(20)	2500	4150(20)	211(13)
C3A	1860(30)	1780(30)	3397(12)	93(7)
C1A	390(50)	2110(70)	3050(30)	160(20)

Table S7. Anisotropic Displacement Parameters ($\text{\AA}^2 \times 10^3$) for $(\text{C}_8\text{H}_{20}\text{N})_2\text{ZnBr}_4$. The Anisotropic displacement factor exponent takes the form: $-2\pi^2[h_2a^*2U_{11}+2hka^*b^*U_{12}+\dots]$.

Atom	U_{11}	U_{22}	U_{33}	U_{23}	U_{13}	U_{12}
Zn01	62.9(8)	62.9(8)	41.4(8)	0	0	0
Br02	132.9(11)	83.2(8)	86.6(9)	-31.8(5)	0	0
N003	83(7)	61(5)	51(5)	0	0	0
C004	250(20)	101(10)	120(12)	-51(9)	0	0
C006	106(10)	92(9)	91(9)	-8(8)	0	0
C2	220(20)	260(20)	147(19)	0	0	0
C1	166(15)	172(15)	167(15)	0	-4(5)	0
C3	208(15)	219(15)	205(15)	0	-4(10)	0

Atom	U ₁₁	U ₂₂	U ₃₃	U ₂₃	U ₁₃	U ₁₂
C3A	96(10)	97(10)	85(9)	-11(7)	-11(7)	12(8)
C1A	160(20)	170(20)	170(20)	-7(10)	-10(10)	0(10)

Table S8. Bond Lengths for (C₈H₂₀N)₂ZnBr₄.

Atom Atom	Length/Å	Atom Atom	Length/Å
Zn01 Br02	2.4042(10)	N003 C3A	1.476(18)
Zn01 Br02 ¹	2.4042(10)	N003 C3A ⁴	1.476(18)
Zn01 Br02 ²	2.4042(10)	C004 C006	1.49(2)
Zn01 Br02 ³	2.4042(10)	C1 C3	1.41(4)
N003 C006 ⁴	1.56(2)	C3A C3A ⁵	1.29(5)
N003 C006	1.56(2)	C3A C3A ⁴	1.73(4)
N003 C2	1.31(3)	C3A C3A ⁶	1.15(5)
N003 C3	1.51(2)	C3A C1A	1.47(5)
N003 C3 ⁴	1.51(2)	C3A C1A ⁵	1.75(5)
N003 C3A ⁵	1.476(18)	C1A C1A ⁵	0.70(12)
N003 C3A ⁶	1.476(18)		

Table S9. Bond Angles for (C₈H₂₀N)₂ZnBr₄.

Atom Atom Atom	Angle/°	Atom Atom Atom	Angle/°
Br02 Zn01 Br02 ¹	109.80(3)	C1 C3 N003	124(3)
Br02 Zn01 Br02 ²	109.80(3)	N003 C3A C3A ⁴	54.1(9)
Br02 ³ Zn01 Br02 ²	109.80(3)	N003 C3A C1A ⁵	108(2)
Br02 ¹ Zn01 Br02 ³	109.80(3)	C3A ⁶ C3A N003	67.1(10)
Br02 ¹ Zn01 Br02 ²	108.82(6)	C3A ⁵ C3A N003	64.0(10)
Br02 Zn01 Br02 ³	108.82(6)	C3A ⁴ C3A C1A ⁵	94(3)
C006 ⁴ N003 C006	176.4(18)	C3A ⁵ C3A C1A ⁵	55(2)
C2 N003 C3A	144.1(9)	C3A ⁵ C3A C1A	78(2)
C3 ⁴ N003 C006 ⁴	90.00(5)	C3A ⁶ C3A C1A ⁵	139(2)
C3 N003 C006	90.00(5)	C3A ⁶ C3A C1A	154.6(19)
C3 N003 C006 ⁴	90.00(5)	C1A C3A N003	125(3)
C3 ⁴ N003 C006	90.00(5)	C1A C3A C1A ⁵	23(4)
C3 ⁴ N003 C3	180(3)	C1A ⁵ C1A C3A	102(2)
C004 C006 N003	111.7(16)		

Table S10. Torsion Angles for (C₈H₂₀N)₂ZnBr₄.

A	B	C	D	Angle/°	A	B	C	D	Angle/°
N003	C3A	C1A	C3A ¹	47(2)	C3A ¹	N003	C3A	C3A ²	47.6(18)
N003	C3A	C1A	C1A ¹	47(2)	C3A ³	N003	C3A	C3A ²	-54.3(17)
C006 ²	N003	C3	C1	-91.8(9)	C3A ³	N003	C3A	C1A	-154(3)
C006	N003	C3	C1	91.8(9)	C3A ¹	N003	C3A	C1A	-52(3)
C2	N003	C3A	C3A ¹	132.4(18)	C3A ²	N003	C3A	C1A	-100(3)
C2	N003	C3A	C3A ³	-125.7(17)	C3A ²	N003	C3A	C1A ¹	-83(3)
C2	N003	C3A	C3A ²	179.999(3)	C3A ¹	N003	C3A	C1A ¹	-35(2)
C2	N003	C3A	C1A	80(3)	C3A ³	N003	C3A	C1A ¹	-137(2)
C2	N003	C3A	C1A ¹	97(3)	C3A ²	C3A	C1A	C3A ¹	-16.7(19)
C3	N003	C006	C004	89.9(15)	C3A ³	C3A	C1A	C3A ¹	-64(6)
C3 ²	N003	C006	C004	-89.9(15)	C3A ³	C3A	C1A	C1A ¹	-64(6)
C3A ¹	N003	C3A	C3A ³	101.9(6)	C3A ¹	C3A	C1A	C1A ¹	-0.004(9)
C3A ³	N003	C3A	C3A ¹	-101.9(6)	C3A ²	C3A	C1A	C1A ¹	-16.7(19)
C3A ²	N003	C3A	C3A ³	54.3(17)	C1A ¹	C3A	C1A	C3A ¹	0.004(11)
C3A ²	N003	C3A	C3A ¹	-47.6(18)					

Table S11. Fractional Atomic Coordinates ($\times 10^4$) and Equivalent Isotropic Displacement Parameters ($\text{\AA}^2 \times 10^3$) for (C₈H₂₀N)₂Zn_{0.7}Mn_{0.3}Br₄. U_{eq} is defined as 1/3 of the trace of the orthogonalised U_{ij} tensor.

Atom	x	y	z	U(eq)
Zn0	0.7500	0.2500	0.2500	0.057
Br02	0.9666	0.2500	0.3374	0.102
N003	1.2500	0.2500	0.0869	0.066
C004	0.7500	-0.0188	0.5060	0.184
C1	1.3250	0.3272	0.0039	0.353
C2	1.2500	0.5105	0.1716	0.202
C3	0.7500	-0.0809	0.4166	0.155
C5	1.2500	0.4382	0.0840	0.199
C4	1.3219	0.3208	0.1583	0.208
Mn01	0.7500	0.2500	0.2500	0.057

Table S12. Comparison of optical properties and particle size of Mn-based hybrid compounds.

Material	Peak position/FHWM	PLQY	Size	Ref.
$\text{CsMnCl}_3(\text{H}_2\text{O})_2$	618 nm/70 nm	N/A	> 1 cm	1
Cs_3MnBr_5	520 nm/42 nm	49%	N/A	2
$\text{PefH}_2[\text{MnBr}_4]$	521 nm/48 nm	45%	N/A	3
$(\text{C}_8\text{H}_{20}\text{N})_2\text{MnBr}_4$	515 nm/47 nm	85.1%	5 cm	4
$(\text{C}_5\text{H}_6\text{N})_2\text{MnBr}_4$	521 nm/42 nm	95%	20 μm	5
$(\text{C}_{10}\text{H}_{16}\text{N})_2\text{Zn}_{1-x}\text{Mn}_x\text{Br}_4$ ($x = 0-1$)	518 nm/46 nm	0-89.91%	N/A	6
$(\text{CH}_6\text{N}_3)_2\text{MnCl}_4$	650 nm/86 nm	55.9%	10 μm	7
$\text{C}_5\text{H}_5\text{NOMnCl}_2 \cdot \text{H}_2\text{O}$	656 nm/94 nm	24%	1 mm	8
$(\text{NR}_4)_n\text{MnX}_4$	511-539 nm/47-62 nm	< 75%	10-100 mm	9
$(\text{C}_8\text{H}_{20}\text{N})_2\text{MnBr}_4$	517 nm/47 nm	85%	1.5 μm	This work
$(\text{C}_8\text{H}_{20}\text{N})_2\text{Zn}_{0.7}\text{Mn}_{0.3}\text{Br}_4$	517 nm/47 nm	~80%	0.7 μm	This work

N/A: not available

Table S13. Comparison of the thermal stability, photostability of other Mn-emitting hybrid compounds.

Material	Thermal stability	Photostability	Ref.
Cs ₃ Mn _{0.96} Zn _{0.04} Br ₅	120 °C, 84%	N/A	2
(C ₅ H ₆ N) ₂ MnBr ₄	N/A	< 85%/14 Days	5
(C ₉ H ₁₅ N ₃)ZnCl ₄ :Mn ²⁺	120 °C, 65%	N/A	10
[(CH ₃) ₄ N] ₂ Mn _{0.6} Zn _{0.4} Br ₄	N/A	50%/6 Days	11
Cs ₃ Mn _{0.6} Zn _{0.4} Br ₅	120 °C, 50%	50%/6 Days	12
(ABI) ₂ MnBr ₄ :5%Zn ²⁺	120 °C, 61.6%	95%/30 Days	13
(C ₈ H ₂₀ N) ₂ MnBr ₄	125 °C, 70%	~50%/30 Days	This work
(C ₈ H ₂₀ N) ₂ Zn _{0.7} Mn _{0.3} Br ₄	125 °C, 80%	~150%/30 Days	This work

N/A: not available

References

1. H. Xiao, P. Dang, X. Yun, G. Li, Y. Wei, Y. Wei, X. Xiao, Y. Zhao, M. S. Molokeev, Z. Cheng and J. Lin, *Angewandte Chemie International Edition*, 2021, **60**, 3699-3707.
2. B. Su, M. S. Molokeev and Z. Xia, *Journal of Materials Chemistry C*, 2019, **7**, 11220-11226.
3. N. N. Golovnev, M. A. Gerasimova, M. S. Molokeev, M. E. Plyaskin and M. E. Baronin, *Journal of Molecular Structure*, 2022, **1248**, 131468.
4. T. Jiang, W. Ma, H. Zhang, Y. Tian, G. Lin, W. Xiao, X. Yu, J. Qiu, X. Xu, Y. Yang and D. Ju, *Advanced Functional Materials*, 2021, **31**, 2009973.
5. G. Hu, B. Xu, A. Wang, Y. Guo, J. Wu, F. Muhammad, W. Meng, C. Wang, S. Sui, Y. Liu, Y. Li, Y. Zhang, Y. Zhou and Z. Deng, *Advanced Functional Materials*, 2021, **31**, 2011191.
6. G. Zhou, Z. Liu, J. Huang, M. S. Molokeev, Z. Xiao, C. Ma and Z. Xia, *The Journal of Physical Chemistry Letters*, 2020, **11**, 5956-5962.
7. S. Wang, X. Han, T. Kou, Y. Zhou, Y. Liang, Z. Wu, J. Huang, T. Chang, C. Peng, Q. Wei and

- B. Zou, *Journal of Materials Chemistry C*, 2021, **9**, 4895-4902.
8. G. Dai, Z. Ma, Y. Qiu, Z. Li, X. Fu, H. Jiang and Z. Ma, *Inorganic Chemistry*, 2022, **61**, 12635-12642.
 9. Y.-Y. Ma, Y.-R. Song, W.-J. Xu, Q.-Q. Zhong, H.-Q. Fu, X.-L. Liu, C.-Y. Yue and X.-W. Lei, *Journal of Materials Chemistry C*, 2021, **9**, 9952-9961.
 10. X. Zhang, Y. Xiong, K. Liu, N. Wang, L. Fan, W. Li, X. Zhao, J. Zhao and Q. Liu, *Journal of Materials Chemistry C*, 2022, **10**, 13137-13142.
 11. X. Liu, J. Yang, W. Chen, F. Yang, Y. Chen, X. Liang, S. Pan and W. Xiang, *Nano Research*, 2022, DOI: 10.1007/s12274-022-5152-2.
 12. W. Chen, Q. He, Z. He, Q. Wang, J. Ding, Q. Huang, X. Liang, Z. Chen and W. Xiang, *ACS Sustainable Chemistry & Engineering*, 2022, **10**, 5333-5340.
 13. J. Lin, Z. Guo, N. Sun, K. Liu, S. He, X. Chen, J. Zhao, Q. Liu and W. Yuan, *Inorganic Chemistry*, 2022, **61**, 15266-15272.